Charge-density waves in rubidium blue bronze $Rb_{0.3}MoO_3$ observed by scanning tunneling microscopy

C. Brun, J. C. Girard, and Z. Z. Wang
Laboratoire de Photonique et de Nanostructures, CNRS, route de Nozay, 91460 Marcoussis, France

J. Marcus, J. Dumas, and C. Schlenker
Laboratoire d'Etudes des Propriétés Electroniques des Solides, CNRS, Boîte Postal 166, 38042 Grenoble Cedex 9, France
(Received 20 July 2005; revised manuscript received 3 October 2005; published 30 December 2005)

Using low-temperature scanning tunneling microscopy under ultrahigh vacuum, high-resolution topographical images were obtained on a cleaved $(\bar{2}01)$ surface of a rubidium blue bronze ($Rb_{0.3}MoO_3$) single crystal. Only molecular lattice was observed at room temperature. At temperatures of 63 and 78 K, well below the charge density wave (CDW) transition temperature in $Rb_{0.3}MoO_3$, underlying molecular lattice and CDW superlattice were observed simultaneously in topographical constant current images. The amplitude of the CDW modulation is about 0.1 Å along **b**. On the Fourier transform of these images, both main Bragg spots (molecular lattice related) and satellite spots (CDW superlattice related) coexist unambiguously. The average projection of the CDW wave vector on the $(\bar{2}01)$ surface deduced by Fourier transform is consistent with the bulk value obtained previously by other techniques. Our results show clearly that the Peierls phase of the quasi-one-dimensional blue bronze can be studied by STM.

DOI: 10.1103/PhysRevB.72.235119 PACS number(s): 71.45.Lr, 68.37.Ef, 07.79.Cz, 73.20.−r

I. INTRODUCTION

The blue bronzes are low-dimensional conductors exhibiting quasi-one-dimensional (1D) electronic properties and a charge density wave instability below 180 K.[1] They are transition metal oxides with chemical formula $A_{0.3}MoO_3$ (with A=K,Rb). They crystallize in the centered monoclinic $C2/m$ structure with lattice parameters for $K_{0.3}MoO_3$ a=18.25 Å, b=7.560 Å, c=9.855 Å and γ=117.53° (respectively, for $Rb_{0.3}MoO_3$ a=18.94 Å, b=7.560 Å, c=10.040 Å and γ=118.83°).[2] The crystal structure is built with MoO_6 octahedra bilayers, parallel to the $(\bar{2}01)$ cleavage plane. The alkali atoms are located between the bilayers. A bilayer consists of clusters of ten distorted octahedra. A cluster contains three different types of molybdenum sites, namely, Mo(1) related to type I MoO_6 octahedra, Mo(2) (respectively, type II MoO_6) and Mo(3) (respectively, type III MoO_6). The clusters form chains along the $\boldsymbol{b}$ direction (the direction of highest conductivity in $A_{0.3}MoO_3$) through corner sharing. MoO_6 octahedra bilayers result from edge sharing clusters of neighboring chains. However, the type I MoO_6 octahedra do not form continuous chains along the **b** axis. A metal-semiconductor transition,[3] identified as a Peierls transition, occurs around 180 K for $A_{0.3}MoO_3$ with A=K,Rb.[4–9] Although electronic band structure calculations[10] showed that two nondegenerate 1D bands cross the Fermi level, only one CDW wave vector $\boldsymbol{q}_{CDW}$ is experimentally observed. It was proposed that $\boldsymbol{q}_{CDW}$ could be related to the nesting of one band with another by $\boldsymbol{q}_{CDW}=\boldsymbol{k}_{f1}+\boldsymbol{k}_{f2}$ where $\boldsymbol{k}_{f1}$ ($\boldsymbol{k}_{f2}$) is the Fermi wave vector of band 1 (band 2) and this was experimentally confirmed by photoemission experiments.[11–13] From 180 to 100 K the $\boldsymbol{q}_{CDW}$ component along $\boldsymbol{b}^*$ decreases from $0.28\boldsymbol{b}^*$ to the nearly commensurate value $0.25\boldsymbol{b}^*$.

One problem of considerable interest concerns the behavior of the order parameter near the sample surface. Grazing incidence x-ray diffraction study[14] showed, down to 125 K for a range of depth of 20–1000 Å below the $(\bar{2}01)$ cleavage plane of $K_{0.3}MoO_3$, that the CDW wave vector close to the surface is the same as in the bulk. This result has been attributed to weak coupling between MoO_6 octahedra bilayers. On the other hand, in spite of several successes in the study of $(\bar{2}01)$ cleaved surface of blue bronze through scanning tunneling microscopy (STM) at room temperature under ambient pressure,[15–17] many efforts to visualize at low-temperature CDW (through STM) in the blue bronze were unsuccessful up to now. Those attempts were performed in liquid media[18,19] as well as in secondary vacuum with sample cleaved in air.[20] Several interpretations were proposed to explain the absence of CDW modulation in STM experiments. Walter *et al.*[19] suggested that either the CDW is attenuated at the surface or that the CDW in $Rb_{0.3}MoO_3$ is only concentrated on the type-II and -III MoO_6 octahedra and that the amplitude of the modulation is too small to be detected on the sample surface by STM. Tanaka *et al.*[20] proposed that "the conduction electrons do not exist on the surface part of the chains." These interpretations correspond to different mechanisms. It is therefore important to clarify this question by more careful STM experiments. We note that observation of CDW through STM in the molybdenum oxides family was reported recently in bidimensionnal purple bronzes and in η-Mo_4O_{11} on samples cleaved in UHV.[21,22]

The present STM investigation on an *in situ* cleaved $(\bar{2}01)$ surface of a $Rb_{0.3}MoO_3$ single crystal was performed at 63 and 78 K, well below the CDW transition temperature. Both molecular lattice and charge density wave superlattice were observed simultaneously in constant current topographical images. The average CDW wave vector projected on a cleaved $(\bar{2}01)$ plane agrees with the result calculated from the bulk value and the amplitude of modulation of the CDW

superlattice is about 0.1 Å. Similar measurements were performed at room temperature and there was no additional superlattice modulation observed. Our STM results provide direct experimental evidence for the existence of CDW on the $(\bar{2}01)$ surface of $Rb_{0.3}MoO_3$ at low temperature.

II. EXPERIMENTAL SETUP AND RESULTS

The experiments were performed in an UHV-LT-STM system (with Omicron LT-STM head) developed for low-temperature measurements under ultrahigh vacuum conditions, and described elsewhere.[23] Mechanically sharpened Pt/Ir tips were used in these experiments. The durability of the tips, the stability of our system and of the experimental conditions were demonstrated by the ability to get reproducible images with molecular resolution for hours. The quality and stability of the tips were checked frequently by taking spectroscopic data on a gold film before and after imaging the blue bronze. All our measurements were taken at 300, 78, and 63 K in constant current mode. It takes roughly 20 min to acquire an image of a 20 nm $\times$ 20 nm, made of 512 $\times$ 512 pixels, with a scan rate velocity of 20 nm/s. Our typical STM measurement parameters are of +500 mV for the bias voltage (V_b) applied on the sample and of 100 pA for the tunneling current (I_t). We note that the applied bias voltage is about four times the Peierls gap of the blue bronze and that the unoccupied states of the sample are probed in our image.

$Rb_{0.3}MoO_3$ single crystals were grown by the electrolytic reduction technique. Well characterized platelets with dimensions of $2 \times 1 \times 0.2$ mm^3 were selected for this experiment. The sample was pasted directly onto a stainless steel substrate with UHV conductive silver epoxy (H21D). Then a small stainless steel cylinder was glued onto the platelike sample surface, before loading it in the preparation chamber. The cleaved $(\bar{2}01)$ surface is obtained by hitting the stainless steel bar in UHV of 10^{-11} mbar at room temperature. The sample was then introduced into the cold STM head within 10 min. Constant current mode topographical images with high molecular resolution were routinely obtained with LT-STM on a molecularly flat $(\bar{2}01)$ surface of $Rb_{0.3}MoO_3$ at 300, 78, and 63 K.

Figure 1(a) displays a typical STM image with molecular resolution on the $(\boldsymbol{a}+2\boldsymbol{c},\boldsymbol{b})$ plane (area 6.2×7.0 nm^2) obtained in constant current mode (I_t=110 pA, V_b=420 mV) at 63 K. 1D structure of parallel chains along the $\boldsymbol{b}$ direction is clearly seen. The surface lattice vectors $\boldsymbol{b}$ and $\boldsymbol{a}+2\boldsymbol{c}$ are indicated by two arrows and the corresponding centered rectangular unit cell is represented by a rectangle. Due to a lack of calibration of our piezoelectric tip driver at 63 K, the measured lattice parameters are about 20% larger than the previously reported bulk values along the $\boldsymbol{b}$ and $\boldsymbol{a}+2\boldsymbol{c}$ directions. With the bulk lattice data taken from x-ray refinements[24] at 100 K, we recalibrated our raw data images. At variance from STM images of the blue bronze previously reported,[15–17,19,20] Fig. 1(a) reveals an internal structure in the surface unit cell: a primary building block of the chain is formed by a well apparent ball on the left side (corresponding to arrow I in Fig. 1(a)) and a more continuous pattern along the $\boldsymbol{b}$ direction on the right side (corresponding to arrow II in Fig. 1(a)). In some images, we found that the continuous pattern on the right appears as formed by two partly overlapping balls. However, the left ball was always more protruded than the right continuous pattern. With a given state of the apex of the tip, the measured molecular lattice corrugation in our STM experiments is about 0.2 Å along both $\boldsymbol{b}$ and $\boldsymbol{a}+2\boldsymbol{c}$ directions. The distance between the subchains indicated by the first two pairs of left arrows in Fig. 1(a) corresponds to that between the type-I and -II MoO_6 octahedra [see Fig. 1(b)]. It agrees well with the value calculated from the bulk parameters within 10% error. The right pair of arrows indicate the expected position of type-III MoO_6 octahedra chain from the bulk data [see Fig. 1(b)]. Type-III MoO_6 octahedra are therefore not resolved in our STM experiment.

In addition to the molecular resolution, the existence of a superlattice is observed simultaneously in our STM images on the $(\bar{2}01)$ plane of blue bronze. The modulation of the height of type-I and -II MoO_6 octahedra are undoubtedly observed in Fig. 1(a). Figure 1(c) shows a profile drawn along type-I octahedra indicated by the left pair of arrows in Fig. 1(a). This profile reveals periodic peaks, reflecting a periodicity of $\boldsymbol{b}$, and also shows a clear supplementary $4\boldsymbol{b}$ periodicity modulating the height of these peaks. This $4\boldsymbol{b}$ periodic variation of height is equal to the nearly commensurate periodicity existing in blue bronze below 100 K due to the formation of a CDW at low temperature. The amplitude of the modulation indicated by a double arrow in Fig. 1(c) is of 0.1 Å along type-I octahedra. With the same periodicity the modulation along type-II octahedra is also observed but with a lower amplitude of 0.06 Å. In a larger scale image shown in Fig. 2(a), the corresponding 2D fast Fourier transform [Fig. 2(b)] gives more information on the wave vector of this modulation. The brightest spots in Fig. 2(b) represent the main Bragg peaks of the molecular lattice with centered rectangular symmetry. They correspond to a surface unit cell on the $(\bar{2}01)$ plane. Every unit cell consists of four spots in the corner and one spot in the center of the rectangle. For more clarity, the reciprocal unit cell vectors $2\boldsymbol{b}^\star$ and $2(\boldsymbol{a}+2\boldsymbol{c})^\star$ of the surface reciprocal lattice are indicated by two arrows on the right of Fig. 2(b).

By a careful analysis of the Fourier transform, we found that almost all the main Bragg spots are surrounded by four satellite spots. As in x-ray, electron, or neutron diffraction experiments, the satellite spots surrounding the main Bragg spots in the Fourier space are due to a breaking of the translational symmetry related to the existence of a superlattice. However, in our STM experiment, only first-order satellite peaks are clearly distinguishable. In Fig. 2(b) the two observed projected wave vectors $\boldsymbol{q}_{\mathrm{CDW}} = \pm 0.25\boldsymbol{b}^\star + (\boldsymbol{a}+2\boldsymbol{c})^\star$ are indicated by two arrows at the left of the image. We attribute these satellite peaks to the presence of the CDW superlattice. This gives experimental evidence of CDW condensation on the surface of $Rb_{0.3}MoO_3$.

We performed our STM measurements on different samples on selected optically flat terraces. Scan size was varied from 14×15 nm^2 to 28×26 nm^2. The average com

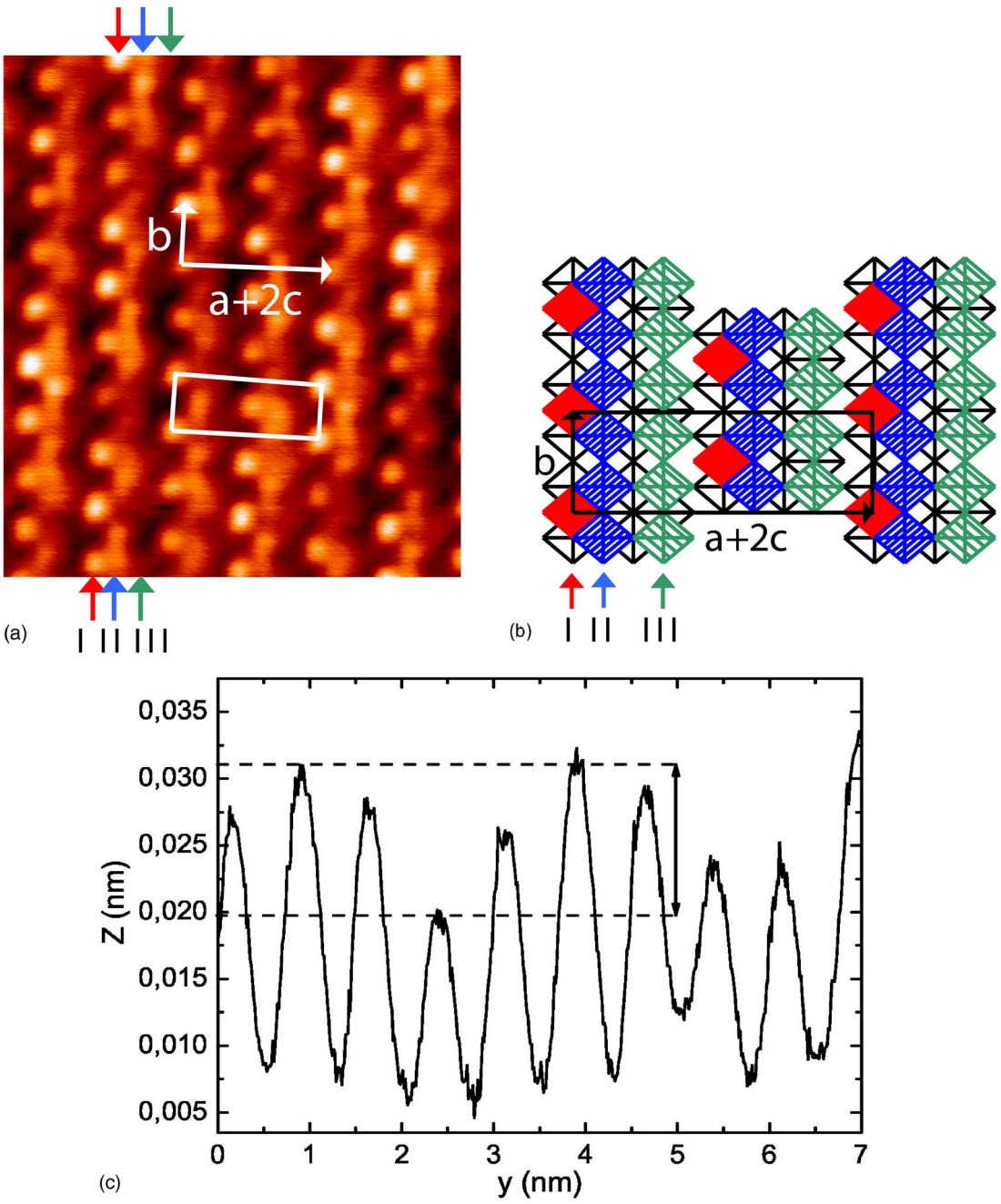

FIG. 1. (Color online) (a) Constant current mode topographical image of 6.2×7.0 nm^2 on a $(\bar{2}01)$ plane of $Rb_{0.3}MoO_3$ at 63 K (raw data image). The applied bias voltage is 420 mV and the setup tunneling current is 110 pA. Surface lattice vectors b and $a+2c$ are indicated by two arrows and the corresponding centered rectangular unit cell is represented by a rectangle. Three pairs of arrows indicate respectively the observed type I and II MoO_6 octahedra and the expected position of type III MoO_6 octahedra. (b) Idealized surface structure of blue bronze in $(\bar{2}01)$ cleavage plane. The filled and dashed square units are MoO_6 octahedra in the first molecular layer. The centers of the filled octahedra (left arrow indicates that they correspond to type-I octahedra) are 0.6 Å higher than the centers of the dark dashed ones (corresponding, respectively, to type-II ones) while the centers of the light dashed ones (corresponding to type-III ones) are 1.1 Å lower than those of the type-II ones [after Walter *et al.* (Ref. 19)]. (c) Profile along the type-I MoO_6 octahedra indicated by left arrows in (a). Different height of the peak represents different local integrated electronic density of states. The periodic variation of height is due to the formation of CDW in blue bronze at low temperature. The amplitude of the modulation indicated by the double arrow is about 0.1 Å.

ponent of $\boldsymbol{q}_{\mathrm{CDW}}$ along the $(\boldsymbol{a}+2\boldsymbol{c})^\star$ direction was found to be close to $(\boldsymbol{a}+2\boldsymbol{c})^\star$ within less than 10% error while the average $\boldsymbol{b}^\star$ direction component was about $0.25\boldsymbol{b}^\star$ with a slightly bigger error. Along the $\boldsymbol{b}$ direction, the amplitude of the modulation of the CDW measured on type I MoO_6 octahedra chain is about half the corrugation of the molecular lattice.

Similar STM measurements have been performed at 300 K, well above the CDW transition temperature in

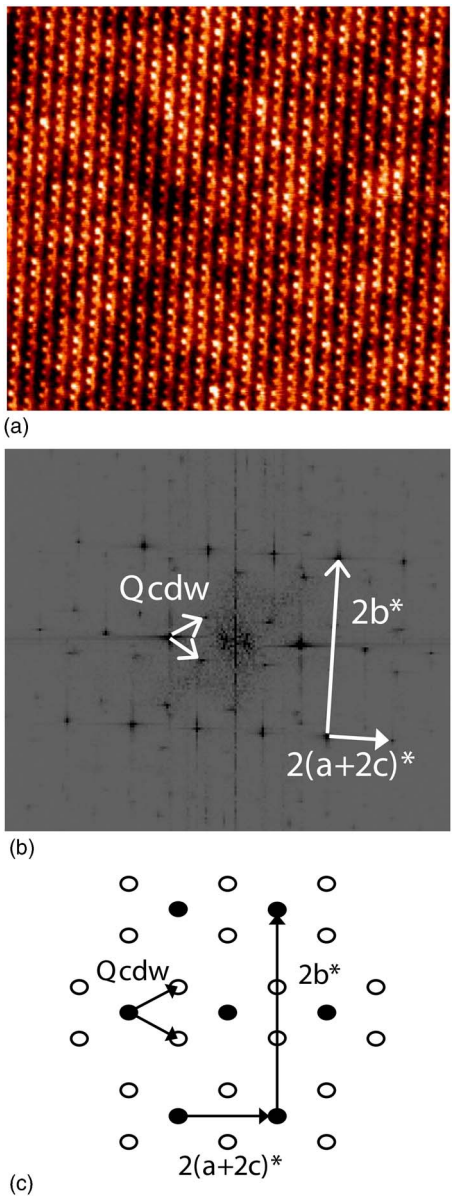

FIG. 2. (Color online) (a) Constant current mode topographical STM image on the $(\bar{2}01)$ plane of $Rb_{0.3}MoO_3$ at 63 K (raw data image). The image area is 28.2×25.9 nm^2. Molecular lattice and CDW superlattice coexist in the image. The applied bias voltage is 420 mV and setup tunneling current is 110 pA. (b) 2D Fourier transform of (a). The brightest Bragg spots correspond to the centered rectangular surface unit cell on the $(\bar{2}01)$ surface of $Rb_{0.3}MoO_3$. A reciprocal unit cell in Fourier space consists of five Bragg spots with unit vectors $2\boldsymbol{b}^\star$ and $2(\boldsymbol{a}+2\boldsymbol{c})^\star$, as indicated by two arrows at the right of the image. Each Bragg spot is surrounded by four satellite spots. This demonstrates the existence of a CDW superlattice with observed projected wave vectors $\boldsymbol{q}_{\mathrm{CDW}} = \pm 0.25\boldsymbol{b}^\star + (\boldsymbol{a}+2\boldsymbol{c})^\star$, giving experimental evidence of CDW condensation on a cleaved surface of $Rb_{0.3}MoO_3$. (c) Diagram showing the respective positions of the atomic lattice Bragg spots (closed circles) and of the CDW superlattice spots (open circles) in the $(\bar{2}01)$ plane, as expected from x-ray and neutron diffraction results at $T < 100$ K.

$Rb_{0.3}MoO_3$. The molecular resolution of the underlying atomic structure has been obtained. However there was no additional superlattice modulation observed. The absence of superlattice modulation in our STM imaging at 300 K supports that the modulation probed at low temperature is CDW phase transition related.

III. DISCUSSION

Previous STM work[15–17,19,20] on a $(\bar{2}01)$ surface of rubidium blue bronze ($Rb_{0.3}MoO_3$) single crystal showed that the observed centered rectangular pattern in STM images reflects the surface unit cell resulting from the projection of the crystal structure on $(\bar{2}01)$. Band-structure calculations in $Rb_{0.3}MoO_3$ (Mozos *et al.*[25]) corroborate that the alkali atoms have no electronic states available near the Fermi level and that they act as donors to fill Mo-O conduction bands with 3 electrons per unit cell. As a result, the alkali atoms do not contribute to the tunneling current and the periodic structure in STM images at room temperature is expected to be due to the uppermost type-I MoO_6 "hump" octahedra. Walter *et al.*[19] postulated that, if the alkali ions would contribute to the image, a large number of surface defects should be observed due to possible nonstoichiometry and to random desorption of rubidium ions from the surface after cleavage. Because they did not observe such defects in their STM measurements, they indeed argued that the centered rectangular periodic structure in STM images is mainly due to the type-I MoO_6 "hump" octahedra or alternatively, in the case of poorer resolution, to a triangular group of one type-I MoO_6 octahedron and two neighboring type-II MoO_6 octahedra [one filled type-I and two dark dashed type-II octahedra forming a triangle as seen in Fig. 1(b)]. The absence of clear surface defects in Figs. 1(a) and 2(a) supports the suggestion of Walter *et al.* that the STM measurement in $Rb_{0.3}MoO_3$ is not sensitive to the rubidium atoms and that the isolated protruded balls are MoO_6 octahedra. The strong hybridization between $4d_{xy}$ electrons of Molybdenum and p electrons of oxygen[25,26] does not allow atomic resolution of Mo and O atoms. Only the MoO_6 octahedra as a whole can be observed in STM imaging.

Our results performed under ultrahigh vacuum are thus consistent with previous data obtained in liquid media[19] and secondary vacuum.[20] However, since they are obtained with an improved resolution, they show better different types of MoO_6 octahedra. Figure 1(b) corroborates that the MoO_6 octahedra when viewed in a $(\bar{2}01)$ plane form a centered rectangular structure. One surface unit cell consists of ten MoO_6 octahedra which are located at different heights and with different effective charges for Mo ions. From their structural and electronic properties, three groups of MoO_6 octahedra are identified in one unit cell: two type-I, four type-II, and four type-III MoO_6 octahedra. The type I MoO_6 octahedra are the uppermost octahedra with respect to the $(\bar{2}01)$ surface and have the periodicity of the unit cell when projected onto the cleavage plane [Fig. 1(b)]. Type-II and -III octahedra occupy the lower sites with a periodicity $0.5b$. Therefore, protruded balls such as the one observed in the

rectangle shown in Fig. 1(a) are attributed to the hump type-I MoO_6 octahedra. The fuzzy part on the right of these protruded balls which presents a more continuous image along the $\boldsymbol{b}$ direction could be attributed to type-II MoO_6 octahedra which are higher than type III. Lateral distances measured between type-I and -II octahedra, as indicated by the first two pairs of left arrows in Fig. 1(a), are in good agreement with the bulk parameters measured by x-ray diffraction within an error of 10%. The deep trough between the more continuous part of the chain and the next set of balls of the adjacent chain may correspond to the type-III MoO_6 octahedra which are absent in Fig. 1(a).

It is now well established that in a topographical STM image measured in constant current mode, the height of the image depends on two different contributions: the electronic density of states and the underlying atomic lattice. Tersoff and Hamann[27] showed that STM experiments provide information not only on the topography of the surface but also on its electronic structure. In blue bronze, differences in heights of the centers of octahedra with respect to the cleavage plane are important: type-I octahedra are 0.6 Å higher than type-II ones while type-III octahedra are 1.1 Å below type-II ones. The charge distribution calculated from structural data show that Mo ions in type-II and -III octahedra have nearly the same density which is larger than that of Mo ions located in type-I octahedra.[24] The tunneling current is proportional to the available integrated local density of states (LDOS) and is exponentially dependent on the tip-sample distance. With a tunneling barrier of 4 eV, a 0.1 Å increase in junction distance will result in a 20% reduction of the tunneling current. The differences in height of MoO_6 octahedra should be reflected in the STM constant current image by the same variation of height, if the local symmetry of the electronic wave functions and the integrated LDOS are identical near each of these octahedra. However, the measured corrugation in the $(\boldsymbol{a}+2\boldsymbol{c})$ direction is about 0.2 Å only as compared to a value of 1.7 Å obtained from crystal structure consideration (see Fig. 3). Indeed differences in height are 0.6 Å between Mo I and Mo II and 1.1 Å between Mo II and Mo III. As comparable DOS are expected on Mo II and III we believe that dominant integrated LDOS contribution in our STM measurements comes from type-I and -II octahedra and that type III do not contribute to the tunneling current. The failure to probe type-III octahedra could be due to the exponential decrease of the tunneling current versus tip-sample distance in the presence of curvature of the STM tip.

The average component of $\boldsymbol{q}_{\mathrm{CDW}}$ along the $(\boldsymbol{a}+2\boldsymbol{c})^*$ direction was found to be close to $(\boldsymbol{a}+2\boldsymbol{c})^*$ within less than 10% error while the average $\boldsymbol{b}^*$ direction component was about $0.25\boldsymbol{b}^*$ with a slightly bigger error. The measured components of the wave vector agree well with the bulk $\boldsymbol{q}_{\mathrm{CDW}}$ components projected onto the cleavage plane taken from bulk or surface measurements. The existence of a CDW at the sample surface is consistent with photoemission experiments[13] at 60 K. It is also consistent with grazing x-ray measurements,[14] which show at $T>125$ K the same CDW wave vector in the surface layers of 2–100 nm as in the bulk.

Since a CDW is associated to a periodic lattice distortion, STM imaging of a CDW system involves both an electronic and a lattice contribution. In the case of the Rb blue bronze, the atomic corrugation observed in our STM measurements is small. It is interesting to estimate whether the bulk atomic displacements would appreciably modify the tunneling current. The accurate data on the bulk mean atomic displacements are given by the x-ray refinements of Schutte *et al.*[24] The lateral components of periodic atomic displacements in $(\bar{2}01)$ cleavage plane, which do not exceed 0.05 Å for Mo(3) (Mo ion of type-III octahedra), are close to the lateral resolution of our measurement and are not detected. The bulk vertical displacement components of the distorted atomic lattice along $[\bar{2}01]$ are of 0.014 and 0.025 Å, respectively, for Mo(2) and Mo(3). This is at least four times less than the modulation of the CDW measured in our experiment on the type-II MoO_6 octahedra chain. We have also taken into account the possibility of measuring by STM the modulation of the Mo(2)-O distances along $[\bar{2}01]$. Again, the bulk value is much less than the observed CDW modulation. Concerning now the type-I MoO_6 octahedra, the Mo(1) displacement is along [121] direction and the vertical component of the bulk atomic displacements with respect to the $(\bar{2}01)$ surface is of 0.01 Å thus ten times smaller than 0.1 Å, the CDW modulation amplitude measured by STM. We therefore conclude that if the amplitudes of the atomic displacements at the surface are comparable to the amplitudes in the bulk, our STM measurement is not sensitive to these periodic displacements for type-I and type-II octahedra. Then the difference in height in Figs. 1(a) and 2(a) along type-II octahedra could represent the different integrated LDOS due to the formation of the CDW at low temperature. This would be consistent

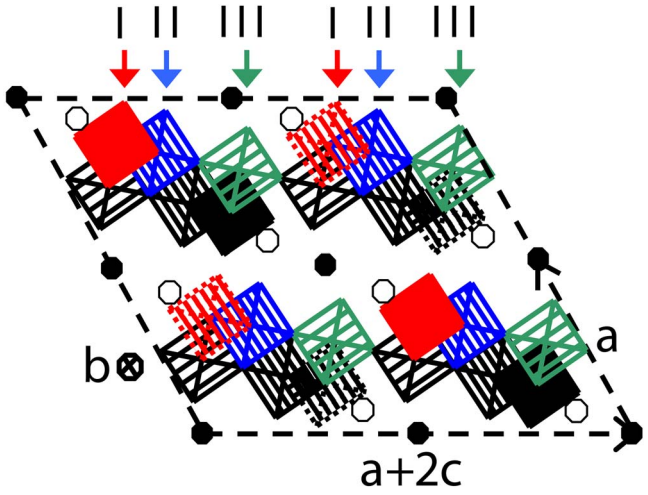

FIG. 3. (Color online) Idealized side view of a single unit cell of blue bronze projected onto the plane perpendicular to the $\boldsymbol{b}$ axis. In the STM experiment, the sample was cleaved *in situ* along $\boldsymbol{a}+2\boldsymbol{c}$ to obtain a $(\bar{2}01)$ surface. Closed circles are the Rb atoms in the uppermost positions. Open circles are the Rb atoms 1.2 Å below the "surface." Each square represents a MoO_6 octahedron with Mo atom located at the center of oxygen octahedron. The three highest octahedra with respect to the "surface" are the dashed squares indicated by the arrows as type I, II, and III ones. Their centers lie at levels 1.8, 2.4, and 3.5 Å below the "surface." Type-I MoO_6 octahedra are the uppermost octahedra.

with the data of Schutte *et al.*[24] at 100 K for *d* electronic density modulation existing on Mo(2) atoms as well as with the more precise first-principles calculations of Mozos *et al.*[25] showing that around the Fermi level the conduction electron density is mostly concentrated on Mo and O atoms of type-II and -III MoO_6 octahedra.

The origin of the measured modulation of height of type-I MoO_6 octahedra is not clear, since according to the bulk data of Schutte *et al.*[24] concerning the valence state on Mo(1) sites, there is no CDW modulation on type-I MoO_6 octahedra. Moreover, first-principle calculations show that the molybdenum ions in the type-I octahedra do not contribute to the DOS around E_f. Therefore integrated LDOS should not contribute to the Mo(1) modulation. In order to understand the contradiction between our STM measurements and other well accepted results in the blue bronze, we may postulate three different mechanisms. First, since the STM image corresponds to the type-I MoO_6 octahedra and not to the Mo I atoms, the strong hybridization between different types of octahedra could be responsible for the CDW modulation observed on type-I MoO_6 octahedra via corner sharing of oxygen atoms. Further numerical simulation should be performed to check this hypothesis. Second, as the applied bias voltage in our STM experiment is as high as 0.5 V, the conventional weak perturbation tunneling model may not be valid. Third, one cannot exclude that there could be a surface reconstruction in the Peierls state of the blue bronze. As a result of the symmetry breaking at the surface, one expects surface reconstruction.[28] If this would be the case, there might exist a surface relaxation driven by the Kohn anomaly on type-I octahedra that would lead to a vertical unexpected CDW-like modulation.

Our STM experiments on the $Rb_{0.3}MoO_3$ blue bronze clearly show that the order parameter of the Peierls transition is non zero at the $(\bar{2}01)$ surface. Previous STM experiments which did not show a CDW modulation at $Rb_{0.3}MoO_3$ surface might be due to a lack of accuracy of the measurements. At variance from STM observations on other low-dimensional systems where the CDW superlattice modulation is typically about 1 Å at low temperature, an unusual small amplitude (0.1 Å) of the CDW superlattice modulation at the cleaved surface of $Rb_{0.3}MoO_3$ is found. For example, in the quasi-two-dimensional purple molybdenum bronze $K_{0.9}Mo_6O_{17}$, the amplitude of the modulation of the CDW superlattice is about 0.4 Å.[21]

Finally, we should mention that when changing the position of the tip on the same optically flat terrace the $\boldsymbol{q}_b$ wave vector was found to deviate from the $0.25\boldsymbol{b}^*$ bulk value on some areas. The inhomogeneity of the wave vector might be related to disorder effects right at the surface[29] and to metastability effects (well known in this compound) at the surface.

IV. CONCLUSION

A charge density wave (CDW) modulation was observed by STM on an *in situ* cleaved surface of the blue bronze $Rb_{0.3}MoO_3$ at the temperature of 63 and 78 K, well below the CDW transition temperature. Both type-I and -II MoO_6 octahedra present a CDW modulation in STM experiment. Molecular lattice and CDW superlattice were observed simultaneously in topographical constant current images. Type-I MoO_6 octahedra are shown as well-defined protruded individual balls while type-II octahedra are characterized by a more continuous pattern. The amplitude of the CDW superlattice modulation measured by STM is about 0.1 Å along $\boldsymbol{b}$. On the Fourier transform of these images, both main Bragg spots (molecular lattice related) and satellite spots (CDW superlattice related) coexist unambiguously. The average projected components of the CDW wave vector measured on a $(\bar{2}01)$ surface agree with x-ray, electron, and neutron diffraction results obtained on bulk samples, as well as with photoemission and grazing x-ray results obtained on cleaved surfaces. Numerical simulations and further experiments should be carried out to clarify the origin of the unexpected CDW-like modulation measured by STM on type-I MoO_6 octahedra and the nature of the inhomogeneity of the CDW wave vector.

ACKNOWLEDGMENTS

This work is supported by Région Ile de France (SESAME project no 1377) and by Conseil Général of Essone. We would like to thank J.P. Pouget, B. Etienne, E. Canadell, P.S. Luo, S. Perraud, P. Mallet and M. Schlenker for useful discussions. The technical assistance of C. David is acknowledged. Laboratoire d'Etudes des Propriétés Electroniques des Solides is associated with Université Joseph Fourier and Institut National Polytechnique de Grenoble.

[1] For a review see *Low Dimensional Electronic Properties of Molybdenum Bronzes and Oxides*, edited by C. Schlenker (Kluwer, Dordrecht, 1989); *Physics and Chemistry of Low Dimensional Inorganic Conductors*, edited by C. Schlenker, J. Dumas, M. Greenblatt, and S. van Smaalen, Vol. 354 of NATO ASI Series (Plenum, New York, 1996); J. Dumas and C. Schlenker, Int. J. Mod. Phys. B **7**, 4045 (1993).

[2] J. Graham and A. D. Wadsley, Acta Crystallogr. **20**, 93 (1966).

[3] W. Fogle and J. M. Perlstein, Phys. Rev. B **6**, 1402 (1972).

[4] G. Travaglini, P. Wachter, J. Marcus, and R. Buder, Solid State Commun. **37**, 599 (1981).

[5] J. P. Pouget, S. Kagoshima, C. Schlenker, and J. Marcus, J. Phys. (Paris), Lett. **44**, L113 (1983).

[6] J. Dumas, C. Schlenker, J. Marcus, and R. Buder, Phys. Rev. Lett. **50**, 757 (1983).

[7] M. Sato, H. Fujishita, S. Sato, and S. Hoshino, J. Phys. C **18**, 2603 (1985).

[8] J. P. Pouget, C. Noguera, A. H. Moudden, and J. Moret, J. Phys. (Paris) **46**, 1731 (1985).

[9] R. M. Fleming, L. F. Schneemeyer, and D. E. Moncton, Phys.

Rev. B **31**, 899 (1985).
[10] W. H. Whangbo and L. F. Schneemeyer, Inorg. Chem. **25**, 2424 (1986).
[11] J. Y. Veuillen, R. C. Cinti, and E. Al Khoury Nemeh, Europhys. Lett. **3**, 355 (1987).
[12] G. H. Gweon, J. W. Allen, R. Claessen, J. A. Clack, D. M. Poirier, P. J. Benning, C. G. Olson, W. P. Ellis, Y-X. Zhang, L. F. Schneemeyer, J. Marcus, and C. Schlenker, J. Phys.: Condens. Matter **8**, 9923 (1996).
[13] A. V. Fedorov, S. A. Brazovskii, V. N. Muthukumar, P. D. Johnson, J. Xue, L-C. Duda, K. E. Smith, W. H. McCarroll, M. Greenblatt, and S. L. Hulbert, J. Phys.: Condens. Matter **12**, L191 (2000).
[14] X. M. Zhu, R. Moret, H. Zabel, I. K. Robinson, E. Vlieg, and R. M. Fleming, Phys. Rev. B **42**, 8791 (1990).
[15] J. Heil, J. Weser, B. Lommel, W. Assmus, and W. Grill, J. Appl. Phys. **65**, 5220 (1985).
[16] D. Anselmetti, R. Wiesendanger, H-J. Güntherodt, and G. Grüner, Europhys. Lett. **12**, 241 (1990).
[17] G. Rudd, D. Novak, D. Saulys, R. A. Bartynski, S. Garofalini, K. V. Ramanujachary, M. Greenblatt, and E. Garfunkel, J. Vac. Sci. Technol. B **9**, 909 (1991).
[18] K. Nomura and K. Ichimura, Solid State Commun. **71**, 149 (1989).
[19] U. Walter, R. E. Thomson, B. Burk, M. F. Crommie, A. Zettl, and J. Clarke, Phys. Rev. B **45**, 11474 (1992).
[20] S. Tanaka, E. Ueda, and M. Sato, Solid State Commun. **87**, 877 (1993).
[21] P. Mallet, K. M. Zimmermann, Ph. Chevalier, J. Marcus, J. Y. Veuillen, and J. M. Gomez Rodriguez, Phys. Rev. B **60**, 2122 (1999).
[22] P. Mallet, H. Guyot, J. Y. Veuillen, and N. Motta, Phys. Rev. B **63**, 165428 (2001).
[23] Z. Z. Wang, J. C. Girard, C. Pasquier, D. Jérome, and K. Bechgaard, Phys. Rev. B **67**, 121401(R) (2003).
[24] W. J. Schutte and J. L. De Boer, Acta Crystallogr., Sect. B: Struct. Sci. **49**, 579 (1993).
[25] J-L. Mozos, P. Ordejon and E. Canadell, Phys. Rev. B **65**, 233105 (2002).
[26] U. V. Waghmare, H. Kim, I. J. Park, N. Modine, P. Maragakis, and E. Kaxiras, Comput. Phys. Commun. **137**, 341 (2001).
[27] J. Tersoff and D. R. Hamann, Phys. Rev. Lett. **50**, 1998 (1983); Phys. Rev. B **31**, 805 (1985).
[28] In a 1D system, due to the existence of soft phonons at $2k_f$, the situation might become more complicated.
[29] One could believe that those alkali atoms represented by closed circles in Fig. 3 may be randomly distributed on a (−201) surface after cleavage. As a result, random surface dipoles could be created that would slightly shift the surface energy bands and hence the effective surface nesting vector leading to inhomogeneities of the CDW surface wave vector measured by STM. Our results concerning these inhomogeneities will be presented in a forthcoming paper.